INVESTIGATIONS OF DIFFERENT RFQ ELECTRODE PROFILES FOR EASY MANUFACTURE*

P. Junior, H. Deitinghoff, A. Harth, W. Neumann, N. Zoubek
Institut für Angewandte Physik, University Frankfurt
Robert-Mayer-Straße 2-4, 6000 Frankfurt am Main, FRG

Abstract

Four electrode profiles are analyzed with respect to field harmonics in the three-dimensional potential caused by profiles, which deviate from the ideal one. Emphasis is given to such electrodes, which can easily be manufactured on a conventional milling machine or a lathe.

The following versions are discussed: 1) the "crankshaft" type, 2) the barrel profile, 3) the trapezoidal electrodes, 4) the finger structure.

Our computational method in calculating the momenta is reported. Finally the influence of relevant coefficients in the potential expansion on particle motion is examplarily studied by means of a 10 - 300 keV proton RFQ linac.

RFQ Profiles

Conventional RFQ linac designs are based on the two term potential[1]. But this involves particular demands on the electrodes. An example was set by the Los Alamos POP experiment[2], where the manufacture of approximately ideal electrodes was accomplished with a computerized milling machine. However, the request for an easier construction becomes obvious. Figs. 1 show principles requiring tools more moderate and in consideration of this the following configurations shall be discussed.

1. The crankshaft structure of figs. 1a, 1b and 2 with constant bore radius $R_1 = R_2$ and rectangularly varying distance R_X resp. R_Y.
2. The cylindrical barrels of figs. 1a, 1b and 3 with constant distance $R_X = R_Y$ and rectangularly varying bores R_1 resp. R_2.
3. Cylindrical rods with constant distance $R_X = R_Y$ and trapeziodally varying bore, as figs. 1a, 1c and 4 illustrate. The principle is realized with $\vartheta = 0.75$ in our proton linac[3,4,5].
4. The fingers with gaps in between, constant bore $R_1 = R_2$ as well as distance $R_X = R_Y$ according to figs. 1a, 1d. This scheme is realized in the GSI MAXILAC[6].

Deviations from the ideal two term case are obvious, thus the performance of higher field moments is the aim of investigations.

3-D Computations

Use is made of the expansion of the potential[1]

$$\Psi(r,\phi,z) = \frac{V}{2} \sum_{\substack{M=0 \\ N=0}}^{\infty} A_{NM} F_{NM}(r,\phi,z) \qquad (1)$$

with

$$F_{NM} = \begin{cases} r^{2M}\cos 2M\phi & N = 0 \\ I_{2M}(Nkr)\cos 2M\cos Nkz & N \geq 1 \end{cases} \qquad (2)$$

and for the determination of the coefficients A_{NM} at given electrode geometry we have composed a computer program. It is based on a three-dimensional least square fit of eq. (1) to the spatial electrode surface. Considering all L relevant coefficients $A_{NM} = X_I$ in arbitrary sequence I = 0...L-1, those are gained as solutions of an inhomogeneous system of L linear equations

$$\sum_{K=0}^{L-1} H_{IK} X_I = R_I \qquad (3)$$

where with eq. (2) the matrix elements are given by surface integrals

$$H_{IK} = \iint I_{IM} \cdot F_{NK} r d\phi dz \qquad (4)$$
$$R_I = \iint F_{NM} r d\phi dz$$

extended over the surface $r = r(\phi,z)$ of the electrodes. According to RFQ symmetry the axial range is only $\pi/2$ and all A_{NM} vanish, when N+M even. Boundary conditions yet undefined in the gap PQ (fig. 1a) are settled by an assumed two-wire potential here. The reliability of results, e. g. what this approximation is concerned, is always checked with the agreement to the voltage on the electrodes, for a precision of about 1 % the order L = 30 of eqs. (3) is mostly required.

Results

Referring to our linac[3,4,5] figs. 5 demonstrate relevant field harmonics occuring with the electrodes 1 - 3 together with the two term coefficients and it's approximation by a harmonic modulation, which can be realized with a milling wheel of constant curvature, however, the increasing cell length in the linac complicates manufacture as well. We have singled out as a representative section the last one at 300 keV. As striking evidence we state that a significant gain in acceleration rate A_{10} compared to the rate with ideal $A_{10}{}^{i}$ at nearly unchanged focusing strength A_{01} takes place in all our cases, however, accompanied by an additive quadrupole term A_{21} and an octupole term A_{12}. Dodekapoles A_{03} and A_{23} turn out too small in all cases to influence particle motion. Neither does jittering caused by A_{30} play a role. Effects on linear motion characterized by the behaviour of the transverse phase advance per period are illustrated in fig. 6. At given transverse phase advance the acceleration rate is more or less significantly improved with all configurations 1 - 3, when compared to the ideal electrode or it's harmonic approximation. This is partially caused by the quadrupole term A_{21} proving helpful when negative. Effects are illustrated by fig. 7, where a particle beam of 10 mA is traced through the linac. The plot shows gains and losses due to A_{21} and A_{12} either in- or excluded , effects seem negligible . It seems that in all our cases the higher momenta are too small to have any negative effect on particle motion, although they usually are not too small for the proper evaluation of all coefficients. Here we can state that for proton linacs admitting large transverse phase advances the ideal surface profile has the disadvantage in construction as well as in acceleration rate at given phase advances. The behaviour of the fingers (s. fig. 1d) is illustrated in fig. 8, where the gap is varied. Together with a strong A_{01} an impressive negative A_{21} term shows up. Now the consequence is that a strong overfocusing happens with our proton data of fig. 6, however, when we consider a typical situation with very heavy ions[6] quite favourable transverse phase advances occur with this structure. Present work is concerned with effects in heavy ion acceleration using all these electrodes, when low charge states demand operation much nearer to the stability limits. Then of course the knowledge of the A_{NM} will be utilized for the determination of peak surface fields.

Computations were carried out at the Hochschulrechenzentrum.

References

[1] I.M. Kapchinskij, V.A. Treplyakov, Prob. Tekh. Eksp. No. 2 (1969) 19
[2] R.W. Hamm et al., Int. Conf. on Low Energy Ion Beams 2, Bath, England April 14 - 17, 1980
[3] A. Schempp et al., IEEE Trans. Nucl. Sci. NS-30 (1983) p. 3536

* Work supported by BMFT

[4] P. Junior et al., ibidem p. 2639
[5] A. Schempp et al., this conference
[6] R.W. Müller et al., this conference
[7] A. Septier, Advances in Electronics and Electron Physics , Academic Press: New York, London, 1961

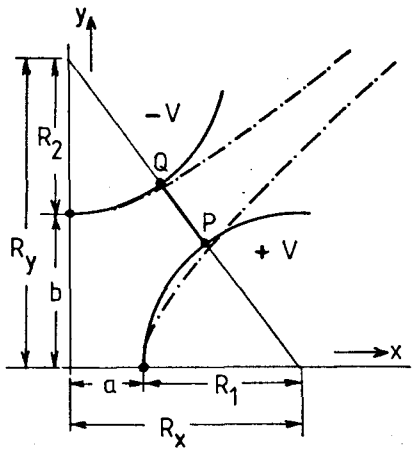

Fig. 1a Transverse cross sections with bore radii R_1 and R_2, dashed hyperbolas correspond to two term case. Note that with types 2 and 3 at constant distance $R_x = R_y$ a larger curvature radius compared to those of the dashed hyperbolas is necessarily involved $R_x = a + b$ usually being taken. In cases 1 and 4 the bore radius agrees with 1.125 a[7]. Peak surface field limitations are not considered.

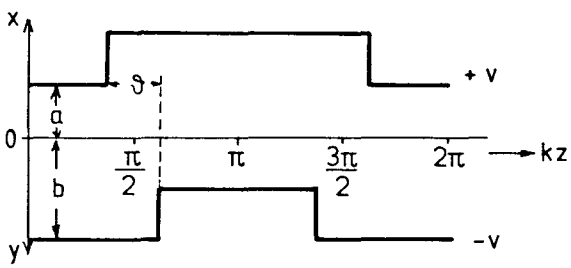

Fig. 1b Longitudinal rectangular cross sections of types 1 and 2

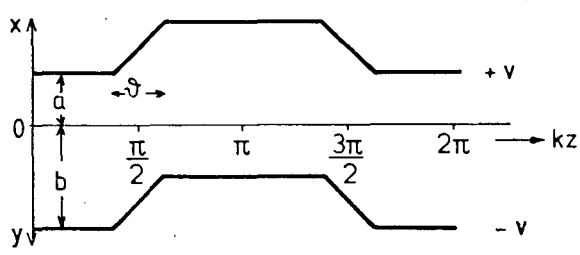

Fig. 1c Longitudinal trapezoidal cross section of type 3

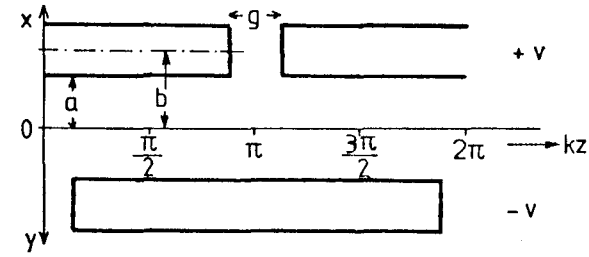

Fig. 1d Longitudinal finger scheme type 4, where acceleration A_{10} is determined by the gap g, lathe required

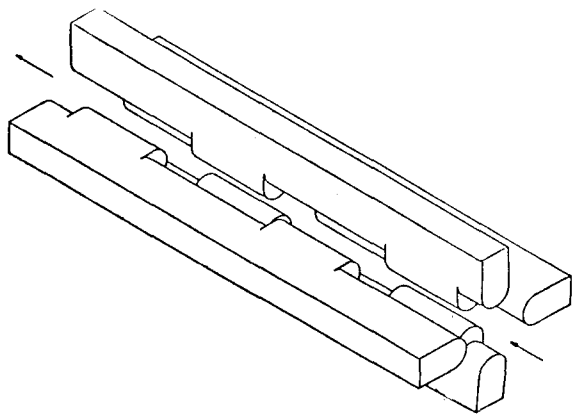

Fig. 2 Sketch of crankshaft, simple milling tool required

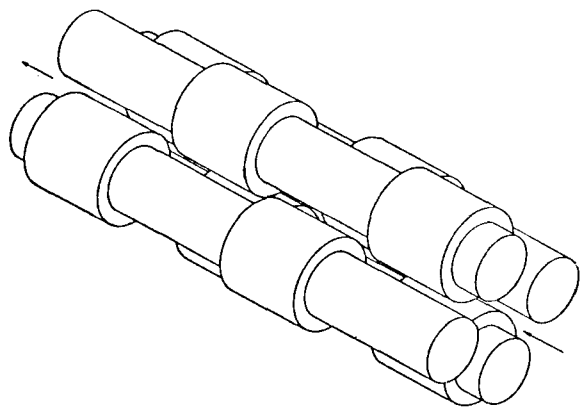

Fig. 3 Sketch of barrels, lathe required

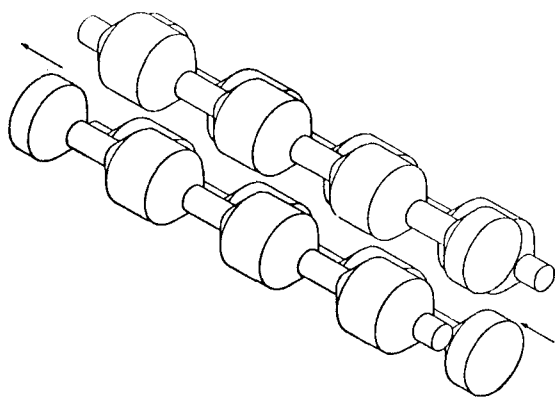

Fig. 4 Sketch of trapezoid, lathe required

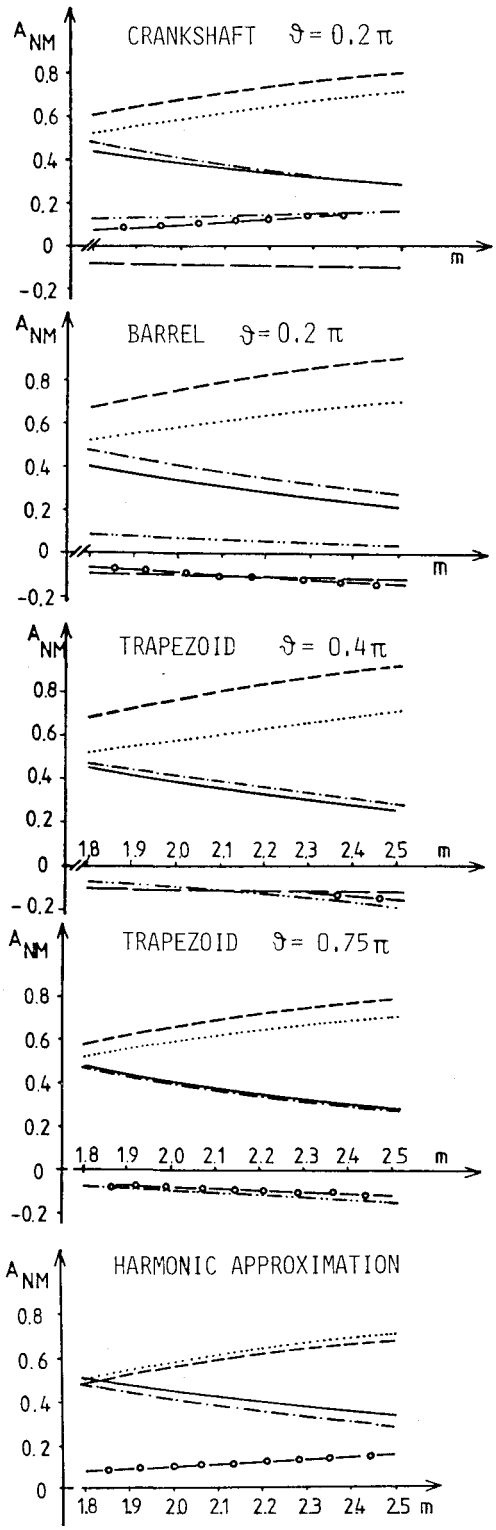

Fig. 5 Field harmonics A_{NM} of representative section with ka = 0.274 versus modulation (a = 3 mm, 108 MHz, 300 keV proton energy)
A_{10}, ideal A_{10}, ideal A_{01}, A_{01}, A_{12}, A_{21}, A_{30}
Normalization $A_{01} = A_{01}/a^2$

$A_{NM} = A_{NM}/I_{2M}\ (Nk\frac{a+b}{2})$

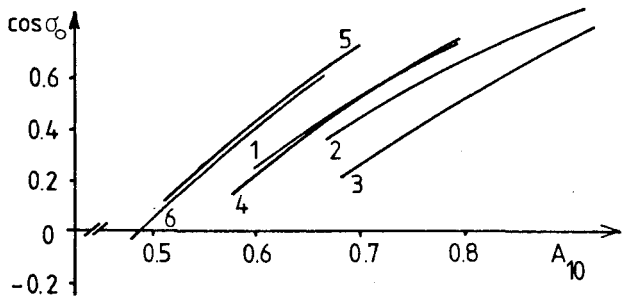

Fig. 6 $\cos\sigma_0$ versus A_{10} of figs. 5, electrode voltage 30 kV
1 crankshaft, 2 barrel, 3 trapezoid $\vartheta = 0.4\pi$, 4 trapezoid $\vartheta = 0.75\pi$, 5 ideal, 6 approximation of 5

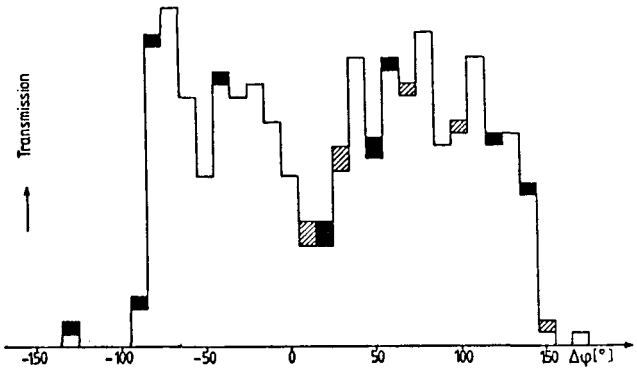

Fig. 7 Gains ■ and losses ▨ of particles due to A_{21} in proton linac[3,4,5]. Transmission about 6 mA, shaper omitted in design, PARMTEQ code, transmission versus phase plotted.

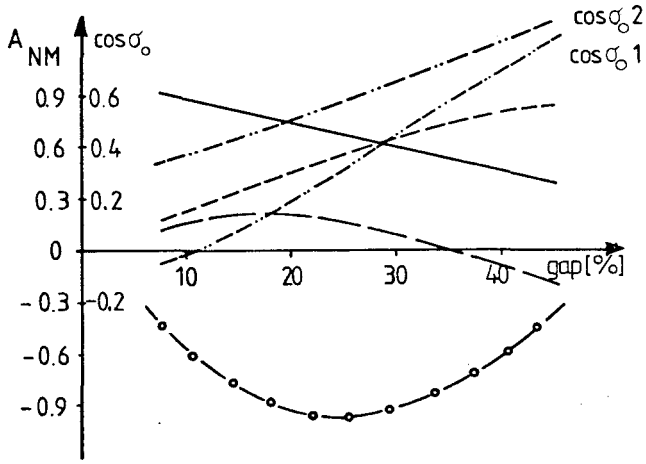

Fig. 8 Field harmonics of fingers type 4 with ka = 0.274 and $\cos\sigma_0$ versus gap in % of $\beta\lambda$, a = 6 mm, 13.5 MHz, 18.75 keV/amu energy, $\cos\sigma_0$ corresponding to
1. 120 kV for ions with ζ/amu = 1/130 resp. 2. 150 kV, 1/208
Legend of curves as in fig. 5